

PACS: 72.80.-r, 72.80.Tm

ISSN 1729-4428 (Print)
ISSN 2309-8589 (Online)

I.M. Voynarovych¹, S.M. Hasynets¹, V.V. Halyan², S.I. Pavley¹, V.V. Lopushansky¹,
V.V. Rubish¹, O.O. Gomonnai³

Characterization of $(\text{As}_2\text{S}_3)_{1-x}(\text{Bi}_2\text{S}_3)_x$ glasses by DC conductivity

¹*Institute of Electron Physics, Nat. Acad. Sci. Ukr., Uzhhorod, Ukraine, voynar@ukr.net*

²*Department of Experimental Physics, Information and Education Technologies, Lesya Ukrainka Volyn National University, Lutsk, Ukraine*

³*Uzhhorod National University, Uzhhorod, Ukraine,*

We present DC conductivity measurements of newly synthesised and thermally annealed $(\text{As}_2\text{S}_3)_{1-x}(\text{Bi}_2\text{S}_3)_x$ ($0.08 \leq x \leq 0.14$) glasses. X-ray diffraction measurements show that as-prepared As_2S_3 glasses were amorphous and after annealing of the samples nucleation and growth of Bi_2S_3 crystallites in an amorphous matrix occurs. Increasing concentration of bismuth sulfide crystalline inclusions leads to an increase in specific conductivity 10^{-10} – 10^{-3} S/m, and decrease in activation energy from 1.2 eV for As_2S_3 down to 0.95 eV for $(\text{As}_2\text{S}_3)_{1-x}(\text{Bi}_2\text{S}_3)_x$ with $x = 0.14$. Recrystallization of bismuth-containing alloys leads to a sharp increase in specific conductivity, and a decrease in the activation energy that can be explained within the framework of the model of micro-inhomogeneous conductivity or by the percolation mechanism.

Keywords: amorphous chalcogenides, DC conductivity, Bi_2S_3 .

Received 07 April 2025; Accepted 27 August 2025.

Introduction

Chalcogenide glasses are very interesting since these materials exhibit transparency in the near and mid-infrared regions, high linear and nonlinear refractive index, optical memory and photoinduced optical changes as photodarkening or photobleaching [1-6]. Doping and alloying of amorphous As_2S_3 with metals leads to the possibility of fine-tailoring their properties over a wide range [7-10]. From the practical application viewpoint, in particular to comply with environmental requirements, Bi-containing chalcogenides, due to their inherent characteristics, are promising as elements of devices with controlled changes in optical and electrical parameters, in particular in memory devices [9]. Generally, undoped chalcogenide glasses show low values of electrical conductivity, which means a serious limit to their technological applications and to electrical measurements. Adding metals to these amorphous materials, even at very low concentrations, leads to a significant increase in their electrical conductivity and even to a change of the type of conductivity [11, 12]. Furthermore, use of various

techniques such as laser ablation, diffusion-limited growth in metal-chalcogenide composites can lead to the formation of metal chalcogenide nanocrystals embedded in a chalcogenide glass matrix, which can be promising materials in optics, electronics, optoelectronics, and materials science due to unique properties [13, 14].

As reported before, thermostimulated transformations of Bi-containing glasses reveal the presence of two overlapping crystallization subprocesses: at high heating rates mostly the nucleation of Bi_2S_3 crystallites occurs while at slower heating As_4S_4 and As_4S_3 crystallites are additionally formed [15]. At irradiation of $(\text{As}_{1-x}\text{Bi}_x)_2\text{S}_3$ glassy samples with a high Bi content ($x \geq 0.14$) with high power laser light (532 nm, 40 kW/cm²), photochemical reactions occur on the surface of the samples with the formation of structural units containing arsenateions AsO_4^{3-} and sulfateions SO_4^{2-} [16]. Amorphous chalcogenide with incorporated nanoparticles are promising for thermoelectric applications in the moderate temperature range (~ 500 K) [17] and can lead to emission in the near infrared range [18]. The aim of our work is to clarify the behavior of DC conductivity of thermally

annealed $(\text{As}_2\text{S}_3)_{1-x}(\text{Bi}_2\text{S}_3)_x$ glasses.

I. Experimental

$(\text{As}_2\text{S}_3)_{1-x}(\text{Bi}_2\text{S}_3)_x$ glasses ($0.08 \leq x \leq 0.14$) were prepared from previously synthesised As_2S_3 glass and needle-shaped Bi_2S_3 crystals which were loaded in desired amounts into evacuated to 10^{-2} Pa quartz ampoules heated to 1020 K at a rate of 50 K/h with subsequent aging for 3 h and cooling at 30 K/h down to 870 K followed by air quenching.

As_2S_3 and Bi_2S_3 were synthesised from stoichiometric amounts of elemental components (99.999% purity) in rotating quartz ampoules evacuated to 10^{-2} Pa heated up to 920 K for As_2S_3 and 1100 K for Bi_2S_3 .

To investigate the possibility of Bi_2S_3 nanocrystal formation in glass, temperature annealing (220–280°C) of samples of different durations (1–5 hours) was carried out.

X-ray diffraction patterns of the samples were recorded using a DRON-3 diffractometer ($\text{CuK}\alpha$ -radiation). Measurements of optical absorption spectra in the range 0.6–1.2 μm were carried out using a Cary 50 UV-Vis (Varian) spectrophotometer with a Xe pulse lamp source and dual Si diode detectors. Fourier spectrometer IRAffinity-1S (Shimadzu) was used for the investigation of transmission spectra in the range of 2–22 μm . The samples were prepared as parallel-plane plates of 0.59 mm thickness.

For DC electrical conductivity, the glass sample was sandwiched between two gold electrodes and the measurement was performed using a specially designed holder in the temperature range 293–440 K. A B7-30 electrometer connected to a simple electrical circuit was used to measure the DC electric current I_{dc} . The DC conductivity σ_{dc} is given by

$$\sigma_{dc} = dI_{dc}/U_{dc}S \quad (1)$$

where I_{dc} is the measured current, U_{dc} is the applied voltage, d is the thickness of the sample with the cross-section S .

II. Results and discussion

Bismuth sulfide nanocrystals were formed by recrystallizing rapidly quenched $(\text{As}_2\text{S}_3)_{1-x}(\text{Bi}_2\text{S}_3)_x$ glasses at different annealing conditions (temperature 220–280°C, duration 1–5 hours). The diffraction patterns of the annealed glasses match well with the diffraction data of the pure polycrystalline Bi_2S_3 with Pbnm space group (curve 6, Fig. 1) [19]. The as-prepared glasses were amorphous according to the X-ray diffraction data (curve 1, Fig. 1). Note, that minimal observable effect of formation of Bi_2S_3 crystalline inclusions in an amorphous matrix confirmed by the XRD measurements for the $(\text{As}_2\text{S}_3)_{0.92}(\text{Bi}_2\text{S}_3)_{0.08}$ samples appeared after annealing at 220 C during 1 hour (curve 2, Fig. 1). Annealing of the samples with $x = 0.10$, 0.12 and 0.14 at 220–280 C during 1 hour in a normal atmosphere also resulted in the formation of Bi_2S_3 crystals in the amorphous matrix (Fig. 1).

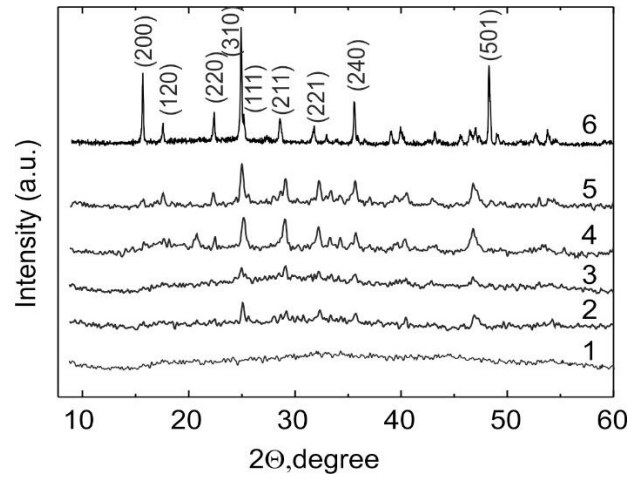


Fig. 1. X-ray diffraction patterns of microcrystalline Bi_2S_3 (6) and composites: $(\text{As}_2\text{S}_3)_{0.86}(\text{Bi}_2\text{S}_3)_{0.14}$, non-annealed (1) and annealed at 250°C, 1 hour (5); $(\text{As}_2\text{S}_3)_{0.92}(\text{Bi}_2\text{S}_3)_{0.08}$ annealed at 220°C, 1 hour. (2), $(\text{As}_2\text{S}_3)_{0.9}(\text{Bi}_2\text{S}_3)_{0.1}$ annealed at 220°C, 1 hour, (3) $(\text{As}_2\text{S}_3)_{0.88}(\text{Bi}_2\text{S}_3)_{0.12}$ annealed at 280°C, 1 hour (4).

Figure 2 (a)–(b) shows the recorded Vis and IR transmittance spectra of As_2S_3 glass and $(\text{As}_2\text{S}_3)_{1-x}(\text{Bi}_2\text{S}_3)_x$ glasses and composites (thickness 0.59 mm) in the wavelength ranges 0.6–1.1 μm and 3–22 μm , respectively. The increasing concentration of bismuth sulfide in chalcogenide glass results in a decrease of the optical bandgap for $(\text{As}_2\text{S}_3)_{1-x}(\text{Bi}_2\text{S}_3)_x$ glasses and therefore leads to a shift of the transmission edge towards longer wavelengths (curve 2–5, Fig. 2a) that coincides with the literature data [10, 20, 21]. The Bi_2S_3 containing glasses (curve 2'–5', Fig. 2a) do not show remarkably different IR transmittance spectrum than the As_2S_3 glass (curve 1, Fig. 2a). Annealing of the composites resulted in a decrease of the infrared transmission near 6–10 μm depending on the time and temperature parameters of the annealing process. Such decrease can most probably be explained by scattering of light.

The dependence of the direct current electrical conductivity of $(\text{As}_2\text{S}_3)_{1-x}(\text{Bi}_2\text{S}_3)_x$ glasses on temperature (Figs. 2–5) was determined using a typical Arrhenius-type relationship

$$\sigma_{dc} = \sigma_0 \exp\left(-\frac{\Delta E_\sigma}{kT}\right) \quad (2)$$

where σ_0 expresses the pre-exponential factor as well as the charge carrier mobility and the density of states, ΔE_σ is the activation energy for the DC conductivity, T is temperature and k is the Boltzmann's constant.

According to the Mott-Davis model, which considers hopping conduction in chalcogenide glasses between localized states within the band gap, in particular, near the Fermi level [22], not only the energy bands exhibit tails, but also some energy states exist near the center of the gap, originating from lattice defects, such as valence alternation pairs and dangling bonds.

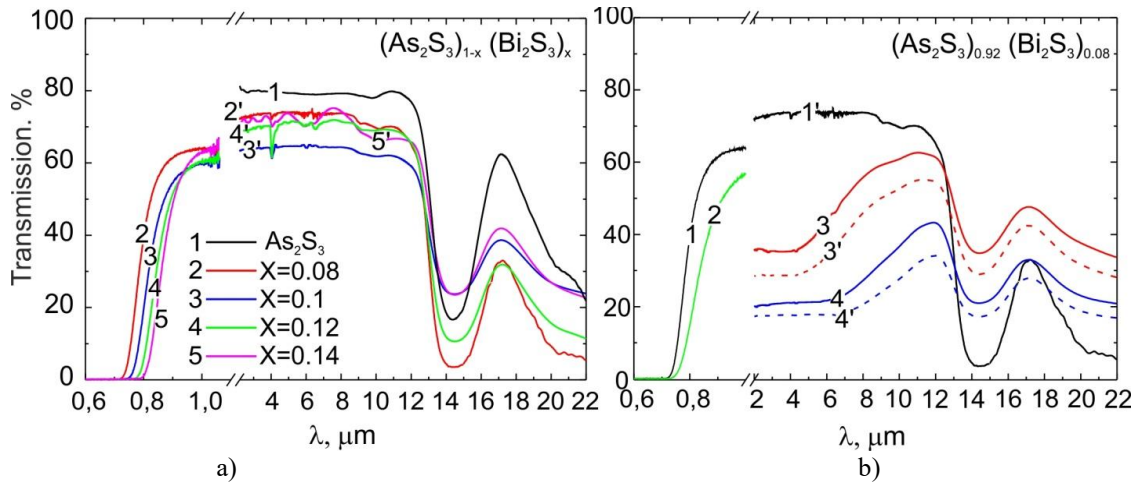


Fig. 2. Vis and IR transmittance spectra of $(As_2S_3)_{1-x}(Bi_2S_3)_x$ glasses: a) non-annealed samples with thickness 0.59 mm. b) Vis and IR transmittance spectra of $(As_2S_3)_{0.92}(Bi_2S_3)_{0.08}$ glasses: non-annealed (1, 1'); annealed at 220°C, 1 hour (2); annealed at 250°C, 1 hour (3), 5 hour (3'), annealed at 280°C, 1 hour (4), 5 hour (4').

These states have the effect of pinning the Fermi level in the center of the mobility gap. In this case, the electrical conduction takes place both in the band tails and in the states near the Fermi level, by means of a phonon-assisted tunneling hopping.

According to Eq. (2), the plots of σ_{dc} versus inverse temperature, shown in Figs. 3-5, are well fitted to a straight line, from which the activation energy can be calculated. From this figure it is obvious that $\ln(\sigma_{dc})$ increases linearly with temperature, the slope of each straight line has a single activation energy value, i.e., DC electrical conductivity is thermally activated over the entire temperature range. Regarding the compositional dependence of the DC electrical properties, as the bismuth sulfide content is increased, the electrical conductivity also increases while the activation energy decreases (Fig. 3). The decrease in the activation energy correlates with the decreasing of the band gap that is revealed in the shift of the optical transmission edge toward the infrared region (Fig. 2a). According to the literature data, introduction of Bi into the amorphous matrix of chalcogenide leads to the appearance of charged defects $-Bi_3^+$ and Bi_4^+ [23], or and [24], where the lower and upper indices mean the coordination number and charge state, respectively. At a low concentration of bismuth, coordination defect pairs $Bi_4^+ - As_1^-$ and $As_4^+ - S_1^-$ are formed [25]. The presence of such defects results in the formation of localized states in the band tails and thereby in the band gap narrowing.

The plots of σ_{dc} versus inverse temperature for annealed glasses are shown in Fig. 4. As can be seen from these plots, annealing of $(As_2S_3)_{1-x}(Bi_2S_3)_x$ glasses with $x = 0.08, 0.1$ and 0.12 for one and three hours leads to a decrease of conductivity while after five hours of annealing for $x = 0.1$ and 0.12 a rapid increase of conductivity occurs. The dependence of the calculated activation energy on the content of bismuth sulfide is shown in Fig. 5. Annealing of $(As_2S_3)_{1-x}(Bi_2S_3)_x$ glasses with $x = 0.08; 0.1$ for three and one hours, respectively, slightly reduces the activation energy because it causes a red shift of the transmission edge (see curve 2, Fig. 2b). In this case, the annealing process leads to local structural ordering by transforming homopolar Bi–Bi and S–S bonds into heteropolar Bi–S bonds, resulting in a creation of new

deep energy states at the band tails.

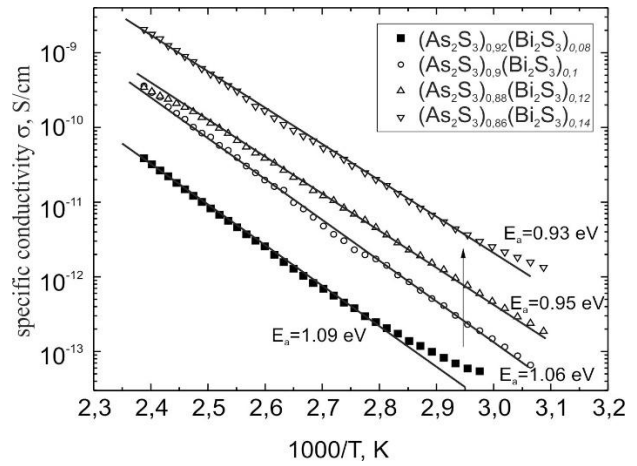


Fig. 3. DC conductivity of non-annealed $(As_2S_3)_{1-x}(Bi_2S_3)_x$ composites depending on temperature.

Further procedure of annealing leads to an increase of the activation energy with a simultaneous decrease of conductivity. Such behavior illustrates the process of nanocrystal growth when the Bi atoms assemble in the crystalline phase of bismuth sulphide and conductivity occurs increasingly through the matrix. For $x = 0.12$ and 0.14 after three and one hours of annealing at 220°C, respectively (Fig. 4, 5), a sharp increase in the specific conductivity and a decrease in the activation energy down to 0.65 eV (Fig. 5) occurs that can be explained within the framework of the micro-inhomogeneous conductivity model or the percolation mechanism [26, 27 and references therein]. When two semiconductor materials with different doping types (p -type As_2S_3 and n -type Bi_2S_3) are connected, a space charge region (also known as a depletion region) is formed at the interface due to the diffusion of charge carriers, in our case from Bi_2S_3 due to concentration of charge carriers $n \sim 3 \times 10^{18} \text{ cm}^{-3}$ [28] to As_2S_3 with $n \sim 3 \times 10^{16} \text{ cm}^{-3}$ [22]. If these regions are close enough, they can overlap, leading to changes in the electric field distribution and the overall conductivity of

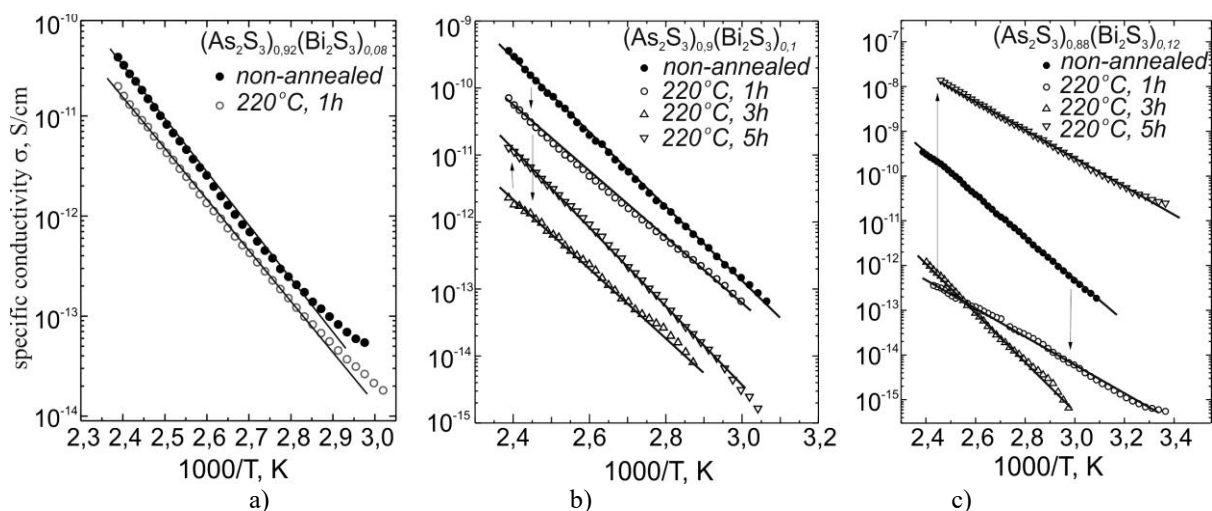


Fig. 4. DC conductivity of annealed bulk $(\text{As}_2\text{S}_3)_{1-x}(\text{Bi}_2\text{S}_3)_x$ composites: a – $(\text{As}_2\text{S}_3)_{0.92}(\text{Bi}_2\text{S}_3)_{0.08}$; b – $(\text{As}_2\text{S}_3)_{0.9}(\text{Bi}_2\text{S}_3)_{0.1}$; c – $(\text{As}_2\text{S}_3)_{0.88}(\text{Bi}_2\text{S}_3)_{0.12}$.

the composite. The energy activation of 0.65 eV supports these mechanisms as it equals to half of the band gap energy $E_g = 1.3$ eV of Bi_2S_3 [28].

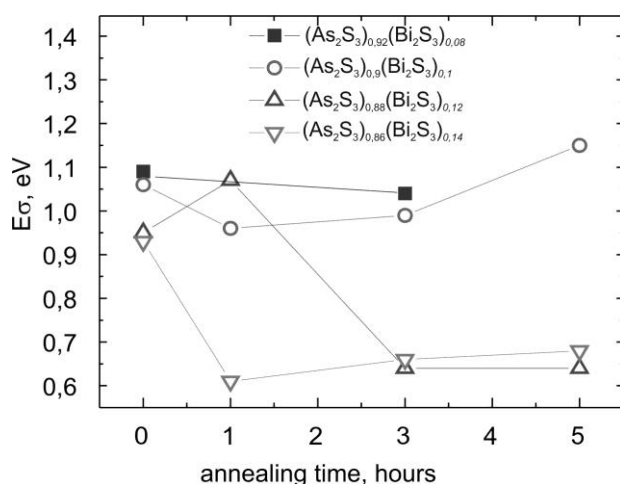


Fig. 5. Activation energy dependence on annealing time for $(\text{As}_2\text{S}_3)_{1-x}(\text{Bi}_2\text{S}_3)_x$ composites.

Conclusions

This paper presents the results of the study of the DC conductivity of as-prepared and annealed $(\text{As}_2\text{S}_3)_{1-x}(\text{Bi}_2\text{S}_3)_x$ glasses ($x = 0.08, 0.1, 0.12, 0.14$). The amorphous structure of the as-prepared glasses was confirmed by XRD. X-ray diffraction measurements show that after the annealing of $(\text{As}_2\text{S}_3)_{1-x}(\text{Bi}_2\text{S}_3)_x$ samples at 220–280°C during 1–5 hours nucleation and growth of Bi_2S_3 crystallites occurs. Optical transmission spectra of glassy samples with different content of bismuth sulfide were studied in the visible and infrared spectral ranges. The increasing amount of bismuth sulfide in the glasses leads to the absorption edge shift towards the long-wavelength range, while measurements in the IR region

do not show remarkably different IR transmittance spectra compared to the As_2S_3 glass.

Measurement of conductivity of the as-prepared glasses of the $(\text{As}_2\text{S}_3)_{1-x}(\text{Bi}_2\text{S}_3)_x$ system in the DC regime showed that introduction of Bi_2S_3 ($0.08 \leq x \leq 0.14$) into the arsenic sulfide matrix leads to an increase in the specific conductivity and a decrease in the activation energy. The dependence of the activation energy on the annealing duration and temperature is calculated. The detected deviations of the experimentally obtained dependences of the activation energy are explained by the growth of nanocrystals. At the beginning of the nucleation and growth of the Bi_2S_3 crystalline phase, the activation energy and the specific conductivity decrease. Further growth results in vanishing of Bi atoms from the matrix that increases the activation energy with a simultaneous decrease of conductivity, and, finally, a sharp increase in the specific conductivity and a decrease of the activation energy down to 0.65 eV reveals the threshold of the percolation mechanism.

Voynarovych I.M. – Ph. D. (Phys. & Math.), Senior Researcher at Department of Materials for Functional Electronics;

Hasynets S.M. – Ph. D. (Chem.), Researcher at Department of Materials for Functional Electronics;

Halyan V.V. – Doctor of Sciences (Phys. & Math.), Professor, Head of Department of Experimental Physics, Information and Educational Technologies;

Pavley S.I. – (Phys. & Math.), Ph. D. student at Department of Materials for Functional Electronics;

Lopushansky V.V. – Ph. D. (Phys. & Math.), Senior Researcher at Department of Materials for Functional Electronics;

Rubish V.V. – Ph. D. (Phys. & Math.), Leading Engineer at Department of Quantum and Plasma Electronics;

Gomonnai O.O. – Doctor of Sciences (Phys. & Math.), Associate Professor at Department of Optics.

- [1] K. Tanaka, K. Shimakawa, *Amorphous chalcogenide semiconductors and related materials* (Springer, 2021); <https://doi.org/10.1007/978-3-030-69598-9>.
- [2] A. Zakery, S. R. Elliott, *Optical properties and applications of chalcogenide glasses: a review*, J. Non-Cryst. Solids, 330, 1 (2003); <https://doi.org/10.1016/j.jnoncrysol.2003.08.064>.
- [3] K. Tanaka, A. Saitoh, *Pulsed light effects in amorphous As_2S_3* , J. Mater. Sci.: Mater. in Electron., 33, 22029 (2022); <https://doi.org/10.1007/s10854-022-08989-x>.
- [4] B. Luther-Davies, *Integrated optics: flexible chalcogenide photonics* Nature Photonics, 8, 591 (2014); <https://doi.org/10.1038/nphoton.2014.169>.
- [5] L. Li, H. Lin, S. Qiao, Y. Zou, S. Danto, K. Richardson, J. D. Musgraves, N. Lu, J. Hu, *Integrated flexible chalcogenide glass photonic devices*, Nat. Photonics, 8 (8), 643 (2014); <https://doi.org/10.1038/nphoton.2014.138>.
- [6] L. Wang, J. Zeng, L. Zhu, D. Yang, Q. Zhang, P. Zhang, X. Wang, S. Dai, *All-optical switching in long-period fiber grating with highly nonlinear chalcogenide fibers*, Appl. Opt. 57, 10044 (2018); <https://doi.org/10.1364/AO.57.010044>.
- [7] M. Šiljegović, S. R. Lukić-Petrović, D. D. Štrbac, N. Celić, I. R. Videnović, *Dependence of chalcogenide glassy $Bi_x(As_2S_3)_{100-x}$ system optical parameters on the doping content*, Acta Phys. Polon. A., 134 (2), 498 (2018); <https://doi.org/10.12693/APhysPolA.134.498>.
- [8] R. Naik, R. Ganesan, K. S. Sangunni, *Optical properties change with the addition and diffusion of Bi to As_2S_3 in the Bi/ As_2S_3 bilayer thin film*, J. Alloys Comp. 554, 293 (2013); <https://doi.org/10.1016/j.jallcom.2012.11.198>.
- [9] T. O. Ajiboye, D. C. Onwudiwe, *Bismuth sulfide based compounds: properties, synthesis and applications*, Results Chem., 3, 100151 (2021); <https://doi.org/10.1016/j.rechem.2021.100151>.
- [10] I. Voynarovych, V. Pinzenik, I. Makauz, M. Shpiyak, S. Kokenyesi, L. Daroczi *Nanocrystallites in Bi–As–S system*, J. Non-Cryst. Solids, 353 (13), 1478 (2007); <https://doi.org/10.1016/j.jnoncrysol.2006.10.073>.
- [11] S. R. Elliott, *Physics of amorphous materials* (Longman, London, 1990).
- [12] M. V. Šiljegović, S. R. Lukić, F. Skuban, D. M. Petrović, M. Slankamenac, *Analysis of conductivity of glasses from the $(As_2S_3)_{100-x}Bi_x$ system in direct and alternating regimes*, JOAM, 11, 2049 (2009);
- [13] B. Karmakar, K. Rademann, A. Stepanov, *Glass Nanocomposites: Synthesis, Properties and Applications* (Elsevier, 2016).
- [14] P. Phogat, Shreya, R. Jha, S. Singh. *Chalcogenide Nanocomposites for Energy Materials*, Engineering and Technology Journal, 9, 4580 (2024); <https://doi.org/10.47191/etj/v9i07.29>.
- [15] V. M. Kryshenik, S. M. Hasynets, A. M. Solomon, V. Y. Loya, V. V. Lopushansky, V. M. Rubish, A. V. Gomonnai, *Temperature-induced phase transformation in $(As_{1-x}Bi_x)_2S_3$ glasses*. Low Temp. Phys., 51 (1), 88 (2025); <https://doi.org/10.1063/10.0034651>.
- [16] Y. Azhniuk, V. Lopushansky, S. Hasynets, V. Kryshenik, A. V. Gomonnai, D. R. T. Zahn, *Photoinduced transformations in $(As_{1-x}Bi_x)_2S_3$ glass observed by Raman spectroscopy*, J. Raman Spectrosc., 55 (5), 637 (2024); <https://doi.org/10.1002/jrs.6658>.
- [17] M. V. Šiljegović, J. Petrović, D. Sekulić, F. Skuban, S. R. Lukić-Petrović, *Impedance response and I–V characteristics of $Bi_6(As_2S_3)_{94}$ and $Bi_7(As_2S_3)_{93}$ at elevated temperature*, J. Mater. Sci.: Mater. in Electron., 31 (17), 14730 (2020); <https://doi.org/10.1007/s10854-020-04036-9>.
- [18] Y. Xu, J. Qi, C. Lin, P. Zhang, S. Dai, *Nanocrystal-enhanced near-IR emission in the bismuth-doped chalcogenide glasses*, Chin. Opt. Lett., 11 (4), 041601 (2013); <https://opg.optica.org/col/abstract.cfm?URI=col-11-4-041601>.
- [19] A. Kyono, M. Kimata, *Structural variations induced by difference of the inert pair effect in the stibnite-bismuthinite solid solution series $(Sb,Bi)_2S_3$* , American Mineralogist, 89, 932 (2004); <https://doi.org/10.2138/am-2004-0702>.
- [20] R. Naik, P. P. Sahoo, C. Sripan, R. Ganesan, *Laser induced Bi diffusion in $As_{40}S_{60}$ thin films and the optical properties change probed by FTIR and XPS*, Opt. Mater., 62, 211 (2016); <https://doi.org/10.1016/j.optmat.2016.10.004>.
- [21] M. Behera, R. Naik, C. Sripan, R. Ganesan, N. C. Mishra, *Influence of Bi content on linear and nonlinear optical properties of $As_{40}Se_{60-x}Bi_x$ chalcogenide thin films*, Current Applied Physics, 19 (8), 884 (2019); <https://doi.org/10.1016/j.cap.2019.05.007>.
- [22] E. A. Davis, N. F. Mott, *Conduction in non-crystalline systems V. Conductivity, optical absorption and photoconductivity in amorphous semiconductors*, Philos. Mag., 22 903 (1970); <https://doi.org/10.1080/14786437008221061>.
- [23] S. R. Elliott, A. T. Steel, *Mechanism for doping in Bi chalcogenide glasses*, Phys. Rev. Lett. 57 (11), 1316 (1986); <https://doi.org/10.1103/PhysRevLett.57.1316>.
- [24] K. L. Bhatia, *Structural changes induced by Bi doping in n-type amorphous $(GeSe_{3.5})_{100-x}Bi_x$* , J. Non-Cryst. Solids, 54 (1), 173 (1983); [https://doi.org/10.1016/0022-3093\(83\)90091-1](https://doi.org/10.1016/0022-3093(83)90091-1).
- [25] R. Golovchak, O. Shpotyuk, A. Kovalskiy, A. C. Miller, J. Čech, H. Jain, *Coordination defects in bismuth-modified arsenic selenide glasses: High-resolution x-ray photoelectron spectroscopy measurements*, Phys. Rev. B., 77 (17), 172201 (2008); <https://doi.org/10.1103/PhysRevB.77.172201>.
- [26] V. V. Kabanov, K. Zagar, D. Mihailovic. *Electrical conductivity of inhomogeneous two component media in two dimensions*, J. Exp. Theor. Phys., 100, 715 (2005); <https://doi.org/10.1134/1.1926432L>.

- [27] R. Landauer, *Electrical conductivity in inhomogeneous media*, AIP Conf. Proc.; 40 (1), 2 (1978); <https://doi.org/10.1063/1.311150>.
[28] O. Madelung, *Semiconductors Data Handbook* (Berlin, Springer, 2004).

І.М. Войнарович¹, С.М. Гасинець¹, В.В. Галян², С.І. Павлей¹, В.В. Лопушанський¹,
В.В. Рубіш¹, О.О. Гомоннай³

Дослідження електрофізичних властивостей стекол $(\text{As}_2\text{S}_3)_{1-x}(\text{Bi}_2\text{S}_3)_x$

¹Інститут електронної фізики НАНУ, м. Ужгород, Україна, voynar@ukr.net

²Кафедра експериментальної фізики, інформаційних та освітніх технологій, Волинський національний університет імені Лесі Українки, Луцьк, Україна

³Ужгородський національний університет, Ужгород, Україна

В даній роботі представлені результати електрофізичних досліджень на постійному струмі синтезованих та термічно відпалених склоподібних композитів $(\text{As}_2\text{S}_3)_{1-x}(\text{Bi}_2\text{S}_3)_x$ ($0,08 \leq x \leq 0,14$). Рентгенівська дифракція показує, що отримані стекла $(\text{As}_2\text{S}_3)_{1-x}(\text{Bi}_2\text{S}_3)_x$ були аморфними, і після термічного відпалу цих зразків відбувається зародження та ріст кристалітів Bi_2S_3 в аморфній матриці. Збільшення концентрації кристалічних включень сульфиду вісмуту приводить до збільшення питомої провідності 10^{-10} – 10^{-3} См/м та зменшення енергії активації електропровідності з 1,2 еВ для As_2S_3 до 0,95 еВ для $(\text{As}_2\text{S}_3)_{1-x}(\text{Bi}_2\text{S}_3)_x$ з $x = 0,14$. Перекристалізація сплавів, що містять вісмут, веде до різкого збільшення питомої провідності та зменшення енергії активації, що можна пояснити в рамках моделі мікронеоднорідної провідності або на основі перколяційного механізму.

Ключові слова: халькогенідні склоподібні напівпровідники, провідність на постійному струмі, Bi_2S_3 .